

MARCIN BĄCZEK^{*)}, JAROSŁAW JANICKI

Institute of Textile Engineering and Polymer Materials
University of Bielsko-Biala
ul. Willowa 2, 43-309 Bielsko-Biala, Poland

Supermolecular structure and selected properties of PA 6/LCO modified fibres

Summary — The objective of the research presented in this paper was to analyze the influence of the LCO Liquid Crystalline Oligoester (LCO) on the supermolecular structure, thermal and mechanical properties of new fibres prepared from PA 6 and LCO blends. Small angle X-ray scattering (SAXS) and wide angle X-ray diffraction (WAXS) methods were used to determine the structure of LCO modifier and the crystal and lamellar structure of PA 6 matrix of the fibres. Based on DSC measurements thermal properties of these fibres were analyzed. Some results of mechanical tests were also presented. All results of investigations into supermolecular structure, thermal and mechanical properties of PA 6/LCO fibres were compared with the results obtained for unmodified PA 6 fibres.

Keywords: supermolecular structure, modified fibres, liquid crystalline oligoester, tensile strength parameters.

STRUKTURA NADCZĄSTECZKOWA I WYBRANE WŁAŚCIWOŚCI MODYFIKOWANYCH WŁÓKIEN PA 6/LCO

Streszczenie — Analizowano wpływ dodatku oligoestru ciekłokrystalicznego (LCO) na strukturę nadcząsteczkową, właściwości termiczne i mechaniczne włókien formowanych z mieszaniny PA 6 i LCO (95/5). Wykorzystując dyfrakcyjne metody SAXS i WAXS zbadano strukturę zarówno modyfikatora LCO włókien poliamidowych (rys. 3), jak i samej matrycy PA 6 (tabela 2). Na podstawie uzyskanych wyników badań rentgenowskich zaproponowano model struktury nadcząsteczkowej modyfikowanych włókien PA 6/LCO (rys. 10), w którym ujawnia się charakterystyczne rozmieszczenie domen modyfikatora w matrycy polimerowej. Na podstawie badań DSC porównano również właściwości termiczne włókien PA 6 oraz modyfikowanych włókien PA 6/LCO (rys. 10, 11) a także wybrane ich właściwości mechaniczne.

Słowa kluczowe: struktura nadcząsteczkowa, włókna modyfikowane, oligoester ciekłokrystaliczny, parametry wytrzymałościowe.

Polyamides are essential materials in fibres production for textiles and technical uses. However, for those fields of applications extremely high strength parameters as well as excellent dimensional stability are required. In order to improve polymer properties they are reinforced with glass fibres or with very high strength and high modulus liquid crystalline polymers LCPs. During the last decades, liquid crystalline polymers were presented as new compounds with superior properties, as compared to conventional polymers. The search for melt-processable LCPs which are miscible with conventional polymers is still a great challenge in polymer science [1]. Blending thermotropic liquid crystalline polymers with semi-crystalline thermoplastic polymers to form *in situ* polymer composites is very attractive because LCP acts a

reinforcing element in the blends and its addition to a polymer matrix has a significant impact on the physical and mechanical properties of the final product [2–7]. It should be noted that the melting temperature of most liquid crystalline polymers is too high for processing semicrystalline thermoplastic polymers. In order to reduce the melting and transition temperature new liquid crystalline oligoesters (LCO), with a much shorter chain than typical liquid crystalline polymers and with flexible units in the main chain, were synthesised, resulting in a decrease of their melting temperature. Due to its relatively low melting temperature LCO can be used as a proper compound for processing with semicrystalline thermoplastic polymers [8–10].

The main goal of the investigations presented in this paper was to determine the influence of the LCO on the supermolecular structure of the fibres which were pre-

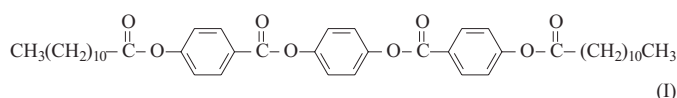
^{*)} Author for correspondence; e-mail:mbaczek@ath.bielsko.pl

pared from the polyamide 6 and liquid crystalline oligo-ester blend (PA 6/LCO). X-ray diffraction methods were used to characterize the supermolecular structure of the polymer matrix of fibres: WAXS was used to characterize crystalline polymorphs and crystallinity of the PA 6 matrix, while parameters of the lamellar structure were extracted from the SAXS patterns. Thermal properties are discussed in the context of Differential Scanning Calorimetry (DSC) results and some results of the mechanical tests are presented as well. The morphological parameters of unmodified PA 6 fibres are included for comparison.

EXPERIMENTAL

Materials

The blend for fibre formation was prepared from PA 6 and liquid crystalline oligoester with 95 % of PA 6 and 5 % of LCO by weight. Commercial PA 6 — Tarnamid T27 (Azoty-Tarnów, Poland) with a density of 1140 kg/m³ and a melt flow index of *MFI* = 12 g/min was used. The LCO was provided by the “Centre of Polymer and Carbon Materials of the Polish Academy of Sciences, Zabrze”. In the molecular structure of LCO, aromatic rings of the mesogen are bonded with ester groups, while the aliphatic end-groups consisting of eleven carbon atoms are connected with the aromatic ring by ester bonds, as shown in Formula (I).



The preparation of the blend consists of three essential stages: blending, extrusion, and annealing at a temperature above T_m of LCO and below T_m of polymer matrix [9, 10].

Formation of fibres

Unmodified PA 6 fibres and fibres from the PA 6/LCO 95/5 blend were formed by using the prototype single-head laboratory extruder. The extruder's head consists of a spinneret with a single hole of diameter $\phi = 0.2$ mm. Fibre-forming materials were melted in a mass cylinder and extruded under the pressure of 0.7 MPa. During the formation process the temperature of the spinneret was set at 230 °C. The fibres were spun with a take-up velocity of 70 m/min.

Methods of testing

— The SAXS/WAXS investigations of the LCO modifier were carried out using the synchrotron beamline of the X33 double focusing camera of the EMBL in Hasylab, at the storage ring DORIS III of the DESY in Hamburg at a

wavelength of 0.15 nm. During the real-time measurements SAXS patterns were simultaneously recorded every 6 seconds giving a temperature resolution of 1 °C per pattern, using a delay line detector. The SAXS intensities were normalized to the intensity of the primary beam and corrected for the detector response. Finally, an averaged melt pattern was subtracted from each curve to eliminate background scattering.

— Static WAXS measurements of powdered raw fibres were performed on a URD6 Seifert diffractometer. $\text{CuK}\alpha$ radiation was used at 40 kV and 30 mA. Monochromatisation of the beam was obtained by means of a nickel filter and a pulse-height analyser. A scintillation counter was used as a detector. Investigations were performed over the range of angles from 5° to 60° using steps of 0.1°. Experimental diffraction patterns were corrected for the polarization and Lorentz factor. After the subtraction of the incoherent scattering and a linear background, the curves were resolved into the crystalline peaks and the amorphous halo using the method described by Hindeleh & Johnson [11, 12] and OPTIFIT software [13]. The fraction of the crystalline phase was calculated from the ratio of the integral intensities of crystalline peaks to the total scattering intensity:

$$x = \frac{I_c}{I_c + I_a} \quad (1)$$

where: I_c — the intensity scattered by the crystalline regions, I_a — the intensity scattered by the amorphous regions.

— Small-angle X-ray scattering investigations for fibres were performed by means of a MBraun camera with conventional Kratky collimation system. The front of the camera was directly mounted on the top of the tube shield of the stabilized Philips PW 1830 X-ray generator. The X-ray tube was operated at a power of 1200 W. $\text{CuK}\alpha$ radiation was used; monochromatisation was performed by a Ni- β filter and a pulse-height discriminator. Scattered radiation was recorded using an acquisition time of 900 s by means of MBraun PSD50 linear position-sensitive detector (1024 channels with a channel-to-channel distance of 52 nm). The experimental SAXS curves were corrected for sample absorption and de-smearred for collimation slit distortion by means of the 3DVIEW MBraun computer program. On the basis of the SAXS curves basic parameters of the lamellar structure of the polymer matrix of fibres were obtained using the correlation function approach [14–16]. The normalized correlation function was calculated, using the OTOKO program [17], from the following equation:

$$\gamma(r) = \frac{\int_0^\infty I(s)s^2 \cos(2\pi \cdot r) ds}{\int_0^\infty I(s)s^2 ds} \quad (2)$$

where: $I(s)$ — the scattering intensity function, r — a distance in real space, s — the modulus of the scattering vector ($s = 2\sin\theta/\lambda$), where λ — the X-ray wavelength and 2θ the scattering angle.

Two-dimensional SAXS measurements were carried out using a 0.5 m long Kiessig-type camera which was equipped with a pinhole collimator and a Kodak imaging plate as a recording medium. The camera was coupled to a Philips PW 1830 X-ray generator (CuK_{α} , operating at 50 kV and 35 mA) equipped with a capillary collimator. To obtain 2D-SAXS patterns exposed imaging plates (exposure time 40 min) were read with a PhosphorImager SI system (Molecular Dynamics).

Thermal properties of the investigated samples were examined by Differential Scanning Calorimetry (DSC). Calorimetric investigations were carried out with a TA Instruments Thermal Analysis System 5100 equipped with a MDSC Calorimeter 2920 and RCS cooling system. The temperature was calibrated with the melting point of indium (156.6 °C) and the enthalpy was calibrated with indium (28.4 J/g). The measurements were performed in the temperature range 20–250 °C, using TA standard aluminium pans, in an atmosphere of nitrogen (flow 40 ml/min) with a heating and cooling rate of 10 °C/min. The weights of the examined samples were about 5 mg. Registration sensitivity was above 0.2 μW . The thermograms were evaluated by means of the Universal V2.6D (TA Instruments) software. DSC curves were presented in a standard arrangement, illustrating the heat flow as the function of sample temperature. The crystallinity index was determined on the basis of the measurements of enthalpy of melting from the following equation:

$$\kappa = \frac{\Delta H}{\Delta H_{100}} \quad (3)$$

where: ΔH — the enthalpy of melting of the fibre, ΔH_{100} — the enthalpy of 100 % crystalline PA 6, the value being assumed is 230.1 J/g [18].

Tensile strength parameters of the fibres were defined by means of the tensile testing machine INSTRON 5544 Single Column. The machine consisted of a press-stretching head for fibres for a static load cell rating ± 10 N with the indication error 1.0 %. The tensile testing machine was connected to the computer equipped with MERLIN software. The measurements were taken at ambient temperature for sample lengths of 10 mm. The tensile speed was 30 $\text{mm} \cdot \text{min}^{-1}$ and 20 tests were made for each sample. On the basis of the measurements the basic mechanical parameters of fibres such as initial modulus breaking tenacity and breaking elongation were determined.

RESULTS AND DISCUSSION

Thermal behaviour and supermolecular structure of the LCO modifier

The thermal behaviour of LCO was analysed using DSC measurements. Table 1 presents the results of our analysis of the DSC heating and cooling curves of the oligoester collected at a rate 10 °C/min.

The values of T_m , ΔH_m and T_i , ΔH_i correspond to the two main endothermal signals, melting and isotropisation, respectively, which are observed in the heating DSC curve. When a cooling run was performed after initial heating, exothermal peaks were observed which were characterized by the values of T_c , ΔH_c and T_{iv} , ΔH_{iv} , respectively.

Table 1. Transition temperatures and enthalpies obtained from DSC measurements during heating and cooling LCO^{a)}

Heating					Cooling			
T_g , °C	T_m , °C	ΔH_m , J/g	T_i , °C	ΔH_i , J/g	T_c , °C	ΔH_c , J/g	T_{iv} , °C	ΔH_{iv} , J/g
40.6	118.7	17.5	156.6	2.3	114.8	11.0	155.0	2.6

^{a)} T_g , T_m , T_c , T_i — glass transition, melting, crystallization and isotropisation temperatures, respectively, ΔH_m , ΔH_c , ΔH_i — the enthalpies of melting, crystallization and isotropisation, respectively.

The results from Table 1 reveal that the LCO modifier exhibits the ability to form a thermotropic mesophase in the temperature range 118–156 °C. The mesophase was detected both during the heating and cooling processes, which is typical for an enantiotropic liquid crystal compound [8].

In order to determine the supermolecular structure of a thermotropic LCO and its changes accompanying the heating to the melt time-resolved SAXS/WAXS measurements during heating and cooling were performed. Fig. 1 presents selected SAXS and WAXS curves of the LCO during heating.

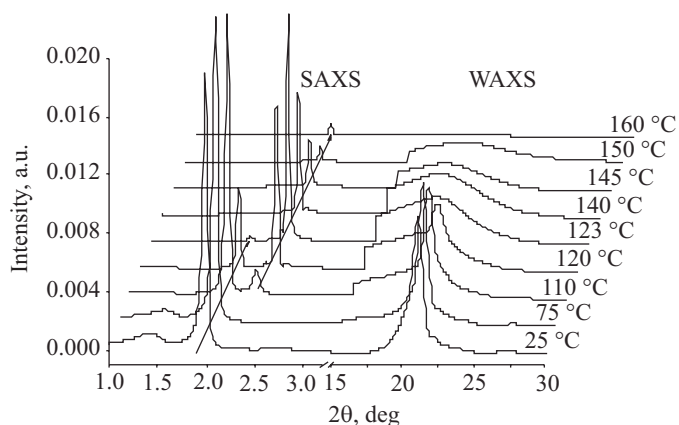


Fig. 1. Time resolved SAXS and WAXS scattering patterns of LCO during heating

The WAXS/SAXS curves exhibit characteristic phenomena: a strong crystalline peak and a very weak amorphous halo in the WAXS data as well as the first diffraction maximum in SAXS curve occurs in the same temperature range (25–123 °C). The crystalline peak in the

WAXS data disappears at 123 °C while the second diffraction maximum in the SAXS data occurs in the temperature range 104–160 °C.

The WAXS patterns registered from 25 °C to 123 °C, involving a strong crystalline peak and a very weak amorphous halo indicate the presence of a well-ordered structure while scattering curves registered at higher temperatures indicate the liquid crystalline state of LCO.

The angular position (2θ) of the peak observed on SAXS curves is connected to the supermolecular structure of the oligoester involving different electron densities of two phases, which are separated by a repeat distance (d -space). The d -space values, based on the position of the first and the second peak (which corresponds to solid crystalline state and liquid crystalline state, respectively) were calculated using Bragg's law and these results are presented in Fig. 2.

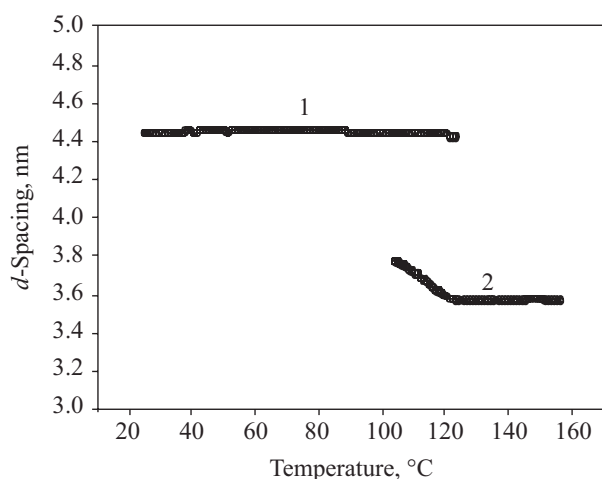


Fig. 2. d -Spacing for LCO: in solid state (1), in liquid crystalline state (2)

Fig. 2 shows that d -space values corresponding to the first peak of the SAXS curves are constant (4.5 nm) and they are characteristic for a well-ordered solid state of the LCO. The values of d -spacing, based on the angular position of the second SAXS peak, steadily decrease from 3.8 nm (104 °C) to 3.6 nm (123 °C) as a result of the increase of chain flexibility during heating. According to our SAXS results the transition occurs at a temperature of 123 °C since the value of d -spacing is constant.

Such SAXS patterns with two diffraction maxima and corresponding changes of d -space values are characteristic of the smectic liquid crystal structure [8, 10, 19].

WAXS studies of supermolecular structure of PA 6/LCO 95/5 fibres

The results of the wide angle scattering measurements were analysed with respect to the crystalline structure of a PA 6 matrix of fibres and the concomitant changes

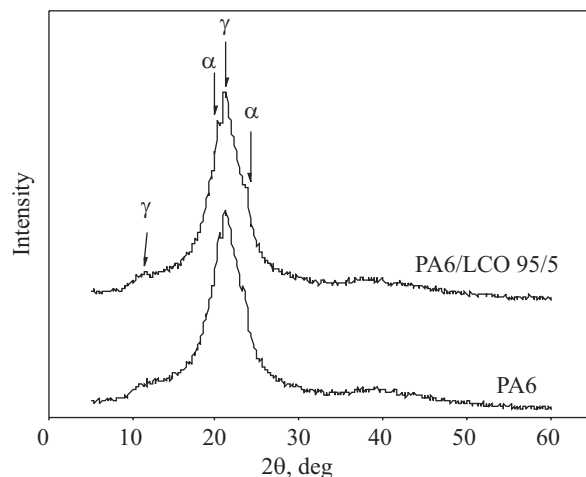


Fig. 3. Comparison of WAXS curves for unmodified and modified polyamide fibres

caused by the addition of a small amount of the LCO modifier; subsequently both sets were compared. The WAXS curves of both PA 6/LCO 95/5 and PA 6 fibres are reported in Fig. 3.

The scattering patterns reveal the existence of the well-known polymorphism of the PA 6 matrix in both samples. Both diffraction curves exhibit the two medium diffraction peaks at $2\theta = 20.3^\circ$ and at $2\theta = 23.7^\circ$, a weak peak at $2\theta = 11^\circ$ and a strong peak at $2\theta = 21.6^\circ$. These two medium peaks are a distinctive feature of the α -crystal polymorph of PA 6 and both the weak and the strong

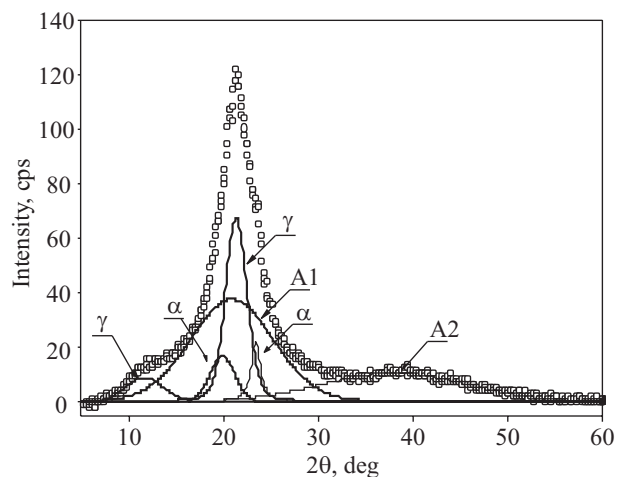


Fig. 4. WAXS curve of PA 6 fibres resolved into individual crystalline peaks and the amorphous components (A1 and A2)

peaks stand for the γ -crystal polymorph of PA 6 [2], which generally is not thermodynamically stable in polyamides and being predominant only under fast cooling conditions during spinning of the fibres. The analysis of the curves reveals that the intensities of all the peaks mentioned above slightly decrease by introducing LCO in the sample. Such changes point to a decrease of the index of

order of the crystalline structure of the polymer matrix for the PA 6/LCO 95/5 fibres. The crystallinity of PA 6 as calculated from equation (1), based on WAXS curves resolved into crystalline peaks and an amorphous halo, is equal to 39 % for PA 6/LCO 95/5 and 41 % for PA 6, respectively. The value of the degree of crystallinity of the modified fibres was calculated only with respect to the PA 6 matrix (Fig. 4 presents WAXS curves of PA 6 resolved into individual crystalline peaks and the amorphous components).

SAXS studies of the supermolecular structure of PA 6/LCO 95/5 fibres

The results of the SAXS experiments are analysed in terms of the lamellar structure of a PA 6 matrix of modified fibres changes as introduced by the LCO additive.

Small angle scattering curves of both modified and unmodified polyamide fibres are presented in Fig. 5.

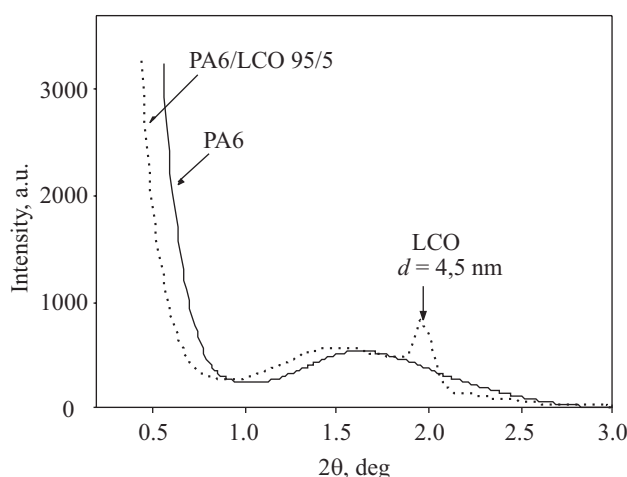


Fig. 5. SAXS curves for PA 6/LCO 95/5 and PA 6 fibres

The SAXS curve of a PA 6 sample exhibits only one wide diffraction peak (1.64°) corresponding to the long period of the lamellar structure of the polyamide. However, the curve of PA 6/LCO 95/5 sample exhibits two distinct peaks: a first one (1.55°) from PA 6 and the second one (1.96°) from the LCO modifier. This clearly points to the fact that the polymer matrix of the modified fibres keeps its lamellar structure in the presence of the oligoester. Moreover, the angular position of the LCO peak in the data of the modified fibre (corresponding to d -space value 4.5 nm) is the same as in the case of the SAXS data of the oligoester (in the solid state) in the absence of the PA 6 matrix (see Fig. 1). This means that the LCO keeps its excellent dimensional stability even in the polymer matrix.

To compare the parameters of the lamellar structure of the PA 6 matrix of both fibres, based on SAXS curves, the correlation functions were calculated from equation (2). A typical correlation function as obtained for PA 6 fibres

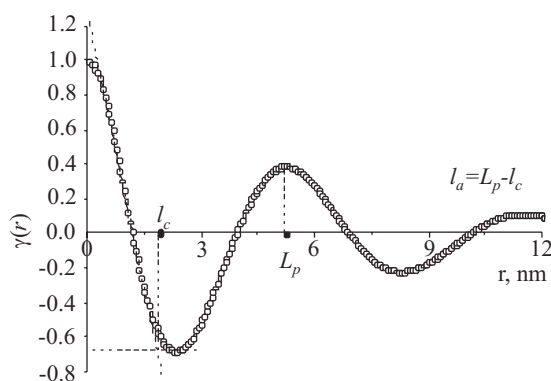


Fig. 6. Correlation function for PA 6 fibres, from which the parameters of lamellar structure are determined

is shown in Fig. 6. The calculation of the long period L_p of the structure is based on the position of the first maximum in the function. Other structural parameters like the crystalline lamellae (l_c) and the amorphous layer thickness (l_a) are also calculated on the basis of this function as shown in Fig. 6. The values of the structural parameters, which are calculated for both investigated fibres are presented in Table 2.

Table 2. The values of parameters of the lamellar structure of PA 6 matrix of investigated fibres, determined by SAXS methods

Sample	L_p , nm	l_c , nm	l_a , nm
PA 6	5.4 *)	5.2	2.0
PA 6/LCO 95/5	5.7 *)	5.3	1.9

*) Long period calculated from Bragg's law based on angular position of the PA 6 peak on the SAXS curve.

The results from Table 2 show that L_p , l_c and l_a values for the modified and the unmodified sample are comparable. It means that the lamellar structure of the polymer matrix of PA 6/LCO 95/5 fibres practically depends on the conditions of the formation of the fibres and is not markedly affected by the presence of the LCO modifier. More details, particularly concerning the distribution of LCO domains in PA 6 matrix of modified fibres are obtained from the 2D-SAXS measurements. The 2D-SAXS patterns of both PA 6 and PA 6/LCO 95/5 fibres are presented in Fig. 7.

Both patterns exhibit symmetrical meridional peaks typical for the polymer matrix. The angular position of the maximum intensity of the peaks is 1.55° and 1.64° for PA 6/LCO 95/5 and PA 6 100, respectively. These results are in excellent agreement with the values of L_p of the lamellar structure of the matrix: 5.7 nm and 5.4 nm for PA 6/LCO 95/5 and PA 6, respectively (see Table 2). In the case of the 2D-SAXS pattern of the LCO modified sample, beside meridional peaks, four diagonal-peaks are observed resulting from the presence of the LCO modifier in the sample. The 2θ position of these peaks and their

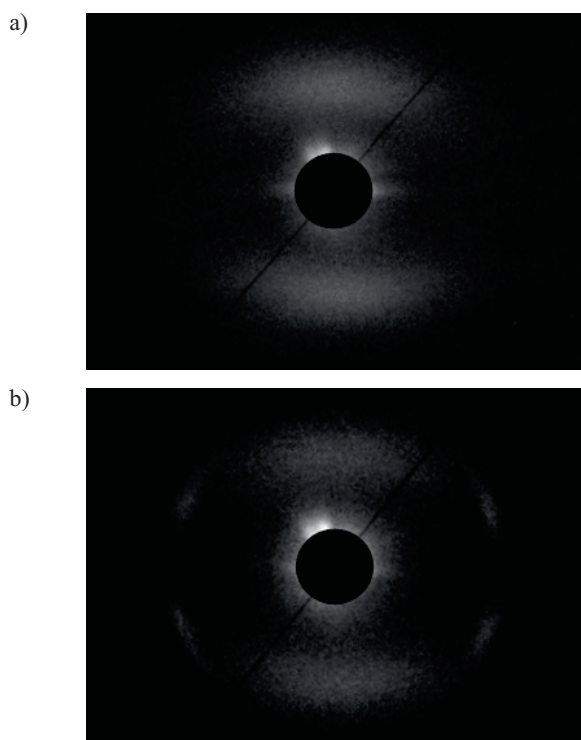


Fig. 7. 2D-SAXS patterns for PA 6 (a) and PA 6/LCO 95/5 (b) fibres

orientation in relation to fibre axe direction were also determined. The 2θ position (1.96°) connected with the d -space of LCO, as expected, is the same as obtained from SAXS curve in Fig. 5. The orientation of the LCO peaks is connected with the distribution of the orientation of the mesogens of LCO in relation to the fibre axis direction. A quantitative estimation of the orientation of the mesogens was obtained by considering an azimuthal plot of SAXS scattering data (for a suitable range of 2θ values). This plot is presented in Fig. 8 and makes clear that the mean angle of the orientation is equal to 70° .

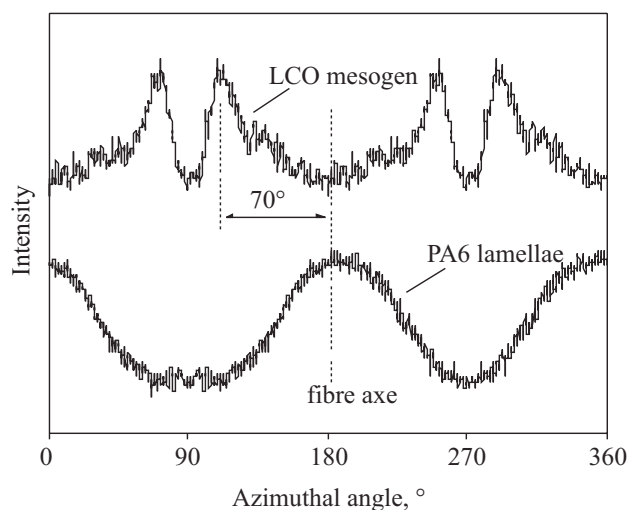


Fig. 8. Azimuthal plot showing the orientation of LCO mesogen and polymer matrix lamellae in PA 6/LCO 95/5 fibres

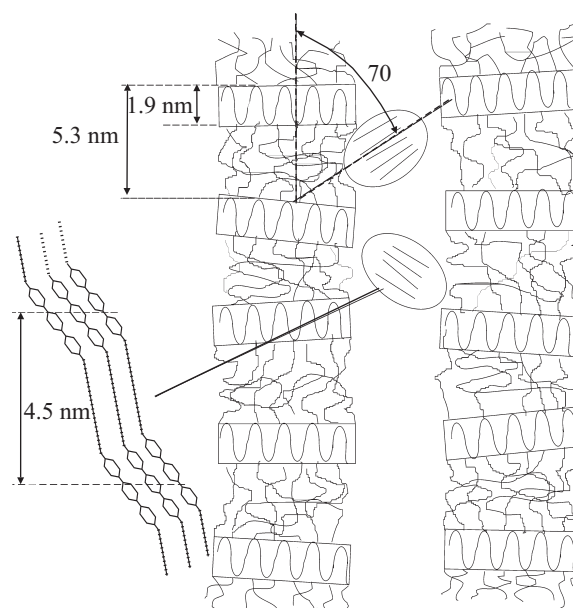


Fig. 9. Proposed model of the supermolecular structure of PA 6/LCO 95/5 fibres based on results derived from SAXS measurements

Based on our results derived from the SAXS measurements, a model of the supermolecular structure of modified fibres is proposed (Fig. 9). This model suggests that the liquid crystalline oligoester domains are distributed into the interfibrillar areas of the polymer matrix as well as slightly slipped between crystalline lamellae (into the amorphous layer). Such a way of distribution of the LCO modifier in PA 6 proves that the LCO in practice only influences the amorphous layers thickness of PA 6 (see Table 2). The proposed model also accounts for the degree of the preferred molecular orientation of the oligoester in the fibres.

Thermal properties of PA 6/LCO 95/5 fibres

The thermal behaviour of the modified PA 6/LCO 95/5 fibres was studied by using differential scanning calorimetry. The results of the DSC measurements are analyzed in terms of changes of the basic thermal parameters of the polymer matrix, such as melting temperature (T_m), enthalpy of melting (ΔH_m), mass degree of crystallinity (κ), crystallization temperature (T_c) and enthalpy of crystallization (ΔH_c) caused by the addition of the LCO modifier.

The shape of the DSC curves (Fig. 10), obtained for both modified and unmodified fibres during heating of the samples in the form "as received" (curve 1 and 2) is similar and they contain only one endothermic peak which illustrates the melting of the crystalline phase of the polymer matrix. The minimum of the endothermic peak occurs at 221.9°C for the modified sample, whereas for the pure polyamide 6 sample it is only very slightly shifted towards a lower value. Additionally, the endothermic effect measured by the value of the enthalpy of

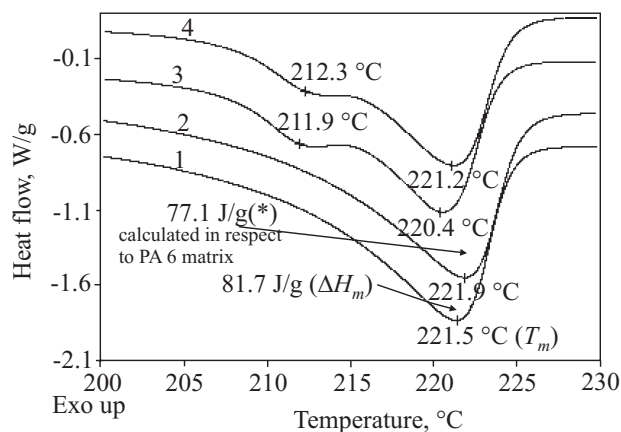


Fig. 10. DSC curves of unmodified (curves 1 and 3) and modified polyamide (curves 2 and 4) fibres during heating at a rate of 10 °C/min registered for: samples in form "as received" (1 and 2), samples after the previous controlled cooling from the melt (3 and 4)

melting (ΔH_m), and calculated only with respect to the polymer matrix, decreases when the LCO modifier is present in the PA 6 matrix. The lower value of ΔH_m indicates that the addition of the modifier causes a slight decrease of the degree of ordering of the supermolecular structure of PA 6. The degree of crystallinity, calculated from equation (3), is 33.5 % and 35.5 % for fibres PA 6/LCO 95/5 and PA 6, respectively.

Another observation resulting from the DSC analysis of the fibres, repeatedly heated after the previous controlled supercooling from the melt (curve 3 and 4), is the presence of two endotherms as compared to one endo-

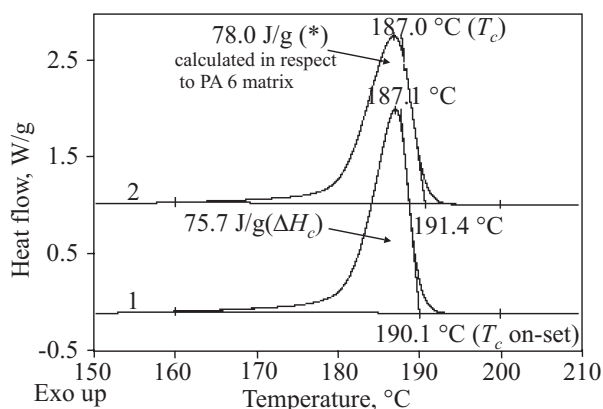


Fig. 11. DSC curves of unmodified (1) and modified (2) polyamide fibres during cooling from the melt at the rate of 10 °C/min

therm in the "as received" samples. The minimum of the first endothermic peak (curve 3 and 4) occurs at a temperature close to 212 °C for both samples and this endotherm probably results from the melting of less perfect crystallites of PA 6.

Next the process of non-isothermal crystallization of the polymer matrix of PA 6/LCO 95/5 fibres was analyzed by comparison of DSC thermograms (Fig. 11) obtained for both unmodified and modified fibres.

Both DSC cooling curves exhibit one exotherm: the crystallization peak. The crystallization peak temperature for both samples is almost the same while differences in the value of the enthalpy of crystallization ΔH_c (calculated only with respect to PA 6) and the onset crystallization temperature ($T_{c\text{ON-SET}}$) are observed. The higher ΔH_c and $T_{c\text{ON-SET}}$ values for the PA 6/LCO 95/5 sample probably result from the heterogeneous nucleation due to the presence of the LCO modifier, which is absent in the crystallization process of the PA 6 matrix.

Mechanical properties of PA 6/LCO 95/5 fibres

The results of the experimental investigation of the effect of LCO modifier on the mechanical properties of polyamide 6 fibres are presented in Table 3.

Table 3. The values of mechanical parameters of unmodified and modified polyamide fibres^{*)}

Sample	M_p , cN/tex	W_r , cN/tex	ϵ_r , %
PA 6 100	1.18	20.5	178.1
PA 6/LCO 95/5	1.99	26.8	184.2

^{*)} M_p , W_r , ϵ_r – initial modulus, breaking tenacity and breaking elongation, respectively.

The comparative analysis of the results shows that presence of the liquid crystalline oligoester has a positive influence on all the investigated parameters of the fibres. The higher values of the initial modulus and of the tenacity, which are observed in the case of PA 6/LCO 95/5 fibres mean that the LCO mesogen acts as a stiff and strong element, which transfers part of the tensions from the matrix of the fibres. Consequently, modified fibres become more stiff and strong in relation to the unmodified PA 6 fibres.

CONCLUSION

This study indicates that the synthesised oligoester which was used as a modifier of PA 6 fibres exhibits the ability of thermotropic mesophase (smectic type) formation. The solid crystalline state of LCO is observed in the temperature range from 25 °C to 123 °C, and the liquid crystalline state in the temperature range 118–156 °C. The crystalline and lamellar structure of the polymer matrix of the fibres formed from the PA 6/LCO 95/5 blend, is not markedly affected by the LCO modifier. The supermolecular structure of the PA 6/LCO 95/5 fibres, proposed in this study, reveals a specific distribution of the LCO domains in the polymer matrix. This specific distri-

bution of the stiff and strong rod-like mesogen of LCO in the PA 6 matrix of the fibres causes a considerable increase in the values of the tensile strength parameters of the fibres.

REFERENCES

1. Takayanagi M., Ogata T., Morkawa M., Kai T.: *J. Macromol. Sci.-Phys. B17* 1980, **4**, 591.
2. Ho J. C., Wei K. H.: *Macromolecules* 2000, **33**, 5181.
3. Hakeni H.: *Polymer* 2000, **41**, 6145.
4. Liang B., Pan L., He X.: *J. Appl. Polym. Sci.* 1997, **66**, 217.
5. Sahoo N. G., Das C. K., Hye-Won Jeong, Chang-Sik Ha: *Macromol. Res.* 2003, **11** (No. 4), 224.
6. Mandal P. K., Bandyopadhyay D., Charkrabarty D.: *J. Appl. Polym. Sci.* 2003, **88**, 767.
7. Kim J. Y., Kang S. W., Kim S. H.: *Fibre Polym.* 2006, **7** (No. 4), 364.
8. Janicki J.: *Acta Phys. Pol. A* 2002, **101**, 761.
9. Janicki J.: *Fibres & Textiles in Eastern Europe* 2003, **11**, No. 5 (44), 101.
10. Bączek M.: "Nanostructure and selected properties of fibres formed from polymeric molecular composites", doctoral dissertation, Bielsko-Biała 2009.
11. Hindeleh A. M., Johnson D. J.: *J. Phys. (D)* 1971, **4**, 259.
12. Hindeleh A. M., Johnson D. J.: *Polymer* 1978, **19**, 27.
13. Rabiej M.: *Polimery* 2002, **47**, 423.
14. Vonk C. G., Kortleve G.: *Kolloid – Z. Z. Polymer* 1967, **220**, 19.
15. Vonk C. G.: *J. Appl. Cryst.* 1973, **6**, 81.
16. Strobl G. R., Schneider M.: *J. Polym. Sci., Polym. Phys. Ed.* 1980, **18**, 1343.
17. Boulin C., Kempf R., Gabriel A., Koch M. H. J.: *Nucl. Instrum. Methods Phys. Res.* 1988, **A249**, 399.
18. <http://athas.prz.rzeszow.pl/> (12.09.2008).
19. Grebowicz J., Wunderlich B.: *J. Polym. Sci., Polym. Phys. Ed.* 1983, **21**, 141.